



HHS Public Access

Author manuscript

Nat Commun. Author manuscript; available in PMC 2014 August 18.

Published in final edited form as:

Nat Commun. 2014 ; 5: 3237. doi:10.1038/ncomms4237.

A cortical-spinal prosthesis for targeted limb movement in paralyzed primate avatars

Maryam M. Shanechi¹, Rollin C. Hu², and Ziv M. Williams²

¹School of Electrical and Computer Engineering, Cornell University, Ithaca, NY, USA

²Department of Neurosurgery, MGH-HMS Center for Nervous System Repair, Harvard Medical School, Boston, MA, USA

Abstract

Motor paralysis is among the most disabling aspects of injury to the central nervous system. Here we develop and test a target-based cortical-spinal neural prosthesis that employs neural activity recorded from pre-motor neurons to control limb movements in functionally paralyzed primate avatars. Given the complexity by which muscle contractions are naturally controlled, we approach the problem of eliciting goal-directed limb movement in paralyzed animals by focusing on the intended targets of movement rather than their intermediate trajectories. We then match this information in real-time with spinal cord and muscle stimulation parameters that produce free planar limb movements to those intended target locations. We demonstrate that both the decoded activities of pre-motor populations and their adaptive responses can be used, after brief training, to effectively direct an avatar's limb to distinct targets variably displayed on a screen. These findings advance the future possibility of reconstituting targeted limb movement in paralyzed subjects.

Brain Machine Interfaces (BMIs) provide a unique opportunity for restoring volitional movement in subjects suffering motor paralysis. Neurons in many parts of the brain including the primary motor and pre-motor cortex, for example, have been shown to encode key motor parameters such as motor intent and ongoing movement trajectory¹⁻⁷. In line with these findings, awake-behaving animals can use the activity from a fairly small number of neurons in the motor cortex to control external devices such as a computer cursor on a screen or a mechanical actuator⁸⁻¹⁹. More recent studies have also demonstrated the possibility of controlling devices such as a robotic arm to produce fluid three-dimensional movements^{9, 11, 12, 17}.

While these approaches have provided key advancements in artificial motor control, another potential goal has been to control the naturalistic movement of one's own limb. This

Users may view, print, copy, download and text and data- mine the content in such documents, for the purposes of academic research, subject always to the full Conditions of use: http://www.nature.com/authors/editorial_policies/license.html#terms

Correspondence and requests for materials should be addressed to Z.M.W. (zwilliams@partners.org).

AUTHOR CONTRIBUTIONS

M.M.S. developed the real-time decoders, performed the analyses, and co-wrote the manuscript. R.C.U performed animal training and recordings. Z.M.W. designed the study, constructed the neural prosthesis, recorded, performed the analyses and wrote the manuscript.

COMPETING INTERESTS STATEMENT

The authors declare that they have no competing financial interests.

prospective capability is particularly attractive in that it could eventually limit the need for mechanical devices to generate movement^{15, 20, 21}. Unlike the control of external devices, however, a distinct problem in attaining limb movement control is that the output of the motor system (e.g. the corticospinal tract and its associated afferents) is generally not explicitly known. For example, when controlling a mechanical device or cursor with a BMI, an experimenter can determine which output commands will move the device up or down. In contrast, the exact combination of successive agonistic and antagonistic muscle contractions naturally used to produce limb movement to different targets in space is difficult to explicitly ascertain or reproduce^{22–25}.

One approach aimed at addressing this problem has focused on using cortical recordings to determine the ongoing trajectory of intended limb movement²⁰. For example, the same muscles that were active during training can be stimulated in sequence to produce muscle contractions that lead to limb movement over a similar trajectory, thus, producing repeated movements to a single object in space. Another approach has also used changes in the activities of individual neurons to direct the contraction force of opposing muscles in order to smoothly move a lever in a line²¹. These approaches have, therefore, provided an important advancement in our ability to mimic the trajectory and velocity of planned movement. However, a fundamental present limitation in these methods is that they are principally aimed at producing movements to a single target at a time or movements within one-dimension. This limitation occurs because the possible combination of distinct muscle contractions significantly increases as the number of possible movement trajectories grows^{24, 25}, especially when considering movement outside one-dimension or in cases where the limb is not narrowly constrained to follow a single repetitive path. While generating such movements can be quite valuable, another compelling goal is the design of a neural prosthetic that can allow subjects to perform movements in higher dimensional spaces and to more than one repetitive target.

Here, we aimed to address this issue from an alternate perspective by focusing on the target of movement itself instead of the intervening ongoing trajectory. We hypothesized that if the intended targets of movement are known, it may be possible to match these with stimulation parameters that elicit limb movements programmed to reach the precise intended targets in space. Specifically, if the planned target of movement can be determined from cortical recordings and if the targets of movement produced by different stimulation sites/parameters can be empirically ascertained, we may be able to elicit limb movement to distinct targets under volitional control. Moreover, this approach would not require an explicit determination of which sequence of muscle contractions or limb kinematics is needed to produce such targeted movement.

Towards this end, we develop a real-time cortical-spinal neural prosthesis in monkeys that infers the planned target of movement based on changes in pre-motor neuronal activity and then matches this information with spinal cord and/or muscle stimulation parameters that elicit movements to the same intended targets on a two-dimensional screen. To test this prosthesis in functionally paralyzed animals, we also devise a novel dual-primate paralysis model that eliminates the potential influence of afferent/efferent pathways such as partially preserved movement or proprioceptive feedback in the tested animals. This is particularly

important, since proximal movement and proprioceptive feedback, which are lost in paralysis but may be preserved by local nerve block, are strongly represented in the motor cortex^{26, 27}. Moreover, healthy subjects can control a BMI more accurately if provided with such feedback²⁶. Finally, we examine two distinct approaches for controlling targeted movements based on either decoded neural population activity or their adaptive response. As an initial proof of concept and to test these two approaches, we focus on producing movements to two possible distinct targets during real-time neural-prosthetic control. Our experiments demonstrate that functionally paralyzed primates are able to precisely reach the different displayed targets on a screen by using cortically controlled stimulation-elicited limb movements within a plane. We compare the performance of neural population decoding versus adaptive neural activity for controlling such targeted limb movements, and discuss the potential benefits and drawbacks for using these techniques.

RESULTS

Dual-Primate Avatar Model for Motor Paralysis

To test volitional motor control in awake-behaving animals without confound of intact efferent/afferent spinal pathways, we first devised a novel dual-primate motor paralysis model. Here, two adult Rhesus monkeys (*macaca mulatta*) were separately designated as either a master or an avatar on different sessions. The monkey functioning as the *master* was responsible for controlling movement based on cortically recorded neural activities, and the other sedated monkey functioned as the *avatar* and was responsible for generating movement based on distal spinal cord and/or muscle stimulations. Since the sedated avatar was a separate animal from the master and therefore had no physiological connection with the master, the master had no direct afferent or efferent influence on the avatar's movement and was, therefore, fully paralyzed from the functional standpoint (Fig. 1). The two monkeys were interchangeably used as the master or the avatar on alternate sessions, meaning that we effectively tested two masters and two avatars in this study.

During each session, the master was seated in a primate chair placed within a radiofrequency shielded recording enclosure. Simultaneous multiple-unit recordings were made from the master's pre-motor cortex using chronically implanted planar multielectrode arrays (NeuroNexus Technologies Inc., MI). Signals were digitized and processed to extract action potentials in real-time by a Plexon workstation (Plexon Inc., TX). The avatar was fully sedated (using a combination of ketamine, xylazine and atropine) and was seated in a separate enclosure. The avatar's limb was attached to a planar, free range-of-motion (360 degree), spring-loaded joystick that controlled a cursor displayed on the master's screen.

All trials during the task began with presentation of a small circular target that was positioned at two random locations on the screen. The radius of the targets displayed to the masters was 3.75 cm, with each target occupying approximately 8% of the screen surface at 24x24 cm. After presentation of a go-cue, the master then had to reach the displayed target by directing a cursor, from the center of the screen to the displayed target, using stimulation-elicited limb movement in the avatar (Fig. 2). The cursor had to occupy the target circumference for 100 ms or more in order for the master to receive reward (see *Methods*).

Decoding Intended Movements Using Neural Population Activity

We first used a population decoding approach that estimated the intended target of movement based on changes in the firing activity of neurons recorded within the master's pre-motor cortex. Prior to performing the real-time neural prosthetic experiments, the spiking activity of all pre-motor neurons in the masters were modeled as an inhomogeneous Poisson process in a training session in which they used the joystick to perform the task^{8, 10, 28}. This target-decoding approach is based on prior work by our group and others showing that multiple targets or target-sequences can be accurately decoded from pre-motor neurons prior to movement (see *Methods*).

We recorded a total of 125 well-isolated pre-motor neurons (11–20 units per session) over 10 sessions. In order to estimate the planned movement prior to its execution, we analyzed the neuronal activity during the target presentation period prior to the go-cue. We find that, of the 125 cells recorded, 64 (51%; one-tailed Z-test; $P < 0.01$; Fig. 3a) significantly predicted which target the animals were intending to move to. When further examining model predictions based on the population activity at different time points, accuracy was $82 \pm 12\%$ (mean \pm s.d.) by 500 ms after target presentation and $95 \pm 10\%$ by 1000 ms after target presentation across sessions consisting of 854 trials. By the time the go-cue was first displayed, mean cross-validated prediction accuracy was $96 \pm 10\%$ (one-tailed *t*-test, $n=10$; $P < 0.01$; Fig. 3b). Training across sessions was performed for an average of 85 ± 19 trials (mean \pm s.d.) or approximately 6 minutes prior to performing the real-time experiments.

Testing Stimulation-Elicited Limb Movements

In order to elicit movement in the avatars, stimulating electrodes were chronically implanted in the cervical spinal cord of both monkeys. Two 16-contact iridium oxide stimulating electrodes (100–500 k Ω) were each inserted at the C5 and C6 levels of both avatars (NeuroNexus). In addition to spinal cord electrode implantation, percutaneous electrodes (100–200 k Ω) were placed in the long and short head of the triceps muscle of avatar #1. This was done in order to provide added range of movements not available by spinal cord stimulation in that particular avatar (see *Methods* for further discussion and *Results*, below).

Prior to running the real-time combined recording-elicitation experiments, the stimulating electrodes were tested under different amplitudes and contact locations in order to determine the range of target locations that can be reached. Specifically, we identified which limb movement direction and amplitude will be produced per stimulation setting and contact location in the avatars and, therefore, to which precise target in space the cursor could reach. Similar to prior reported stimulation experiments in anesthetized animals^{22–24, 29–31}, we tested each contact location at serially incremented amplitudes.

In all cases, stimulation frequency was 200 Hz and pulse width was 0.2 ms with cathodal pulse leading. Stimulation duration was 500 ms and was selected to mimic the time it naturally took the masters to move to and hold a target during the normal joystick movement task (i.e., non-prosthetic controlled). The tested stimulation amplitudes ranged from 10–80 μ A and were incremented by 10–20 μ A intervals per electrode contact. For both avatar 1 and 2, stimulations were tested across all 32 electrode contacts located within the ventral spinal

cord at the C5-6 level (4 mm deep from the dorsal surface and 2 mm lateral from the median sulcus). For avatar 1, stimulations were also tested across 4 acute contacts located within the short- and long-head of the triceps muscle. In this case, stimulation frequency was 200 Hz and pulse width was 0.2 ms with cathodal pulse leading. Stimulation duration was 500 ms. The tested stimulation amplitudes ranged from 100–200 μ A incremented by 10–20 μ A intervals per electrode contact.

We defined the targets of elicited movement based on the angle and amplitude of cursor displacement during the last 100 ms of stimulation. Here, the last 100 ms of stimulation was defined as the target “hold-time” and was required in order for the master to receive reward. On average, each electrode array produced movements over a range of end target locations. These individual clusters ranged in width from approximately 6 to 7 cm. Triceps muscle stimulations were somewhat more confined, producing a cluster of end target locations 3.8 cm wide (Fig. 4a,b).

Of the above tested contact locations and stimulation parameters, two were used for each session and avatar to produce stimulation-induced limb movements. These parameters were chosen to produce movements to targets that were distinct and as radially distant from each other as possible using the available implanted electrodes (in principal, however, and as discussed further below, any other stimulation parameters and corresponding elicited limb movements could be used for the task). The mean angle of separation between the two tested movements was 176 degrees for avatar #1 and 34 degrees for avatar #2 (Fig. 5). For avatar #1, mean path length of movement was 10.3 ± 0.2 cm and mean velocity was 86.4 ± 9.0 cm/sec (mean \pm s.d.). For avatar #2, mean path length of movement was 9.4 ± 0.1 cm and the mean velocity was 59.6 ± 3.0 cm/sec. Mean deviation of movement (i.e. how much the movement trajectory deviated from a straight line) was 1.0 cm for avatar #1 and 3.1 cm for avatar #2.

Real-Time Neural Prosthetic Control of Limb Movement

Based on the above testing, we could now predict the intended target of movement based on recorded pre-motor activity in the master and determine which spinal cord and/or muscle electrode locations and stimulation parameters elicit limb movement to the different targets positioned on the screen. Next, we approximated changes in motor intent with movement production using the master-avatar primates in real-time on a trial-by-trial basis.

As the two targets were displayed in random order on the screen, neuronal activity was continuously recorded from the master and was used to predict trial-by-trial changes in the masters' intended target of movement. Therefore, if neuronal activity recorded during the trial predicted that the master was intending to move to target #1, the system would activate the stimulating electrode in the avatar that was previously observed to produce limb movement to that exact target location. Alternatively, if neuronal activity predicted that the master was intending to move towards target #2, the system would activate another electrode that produced a movement towards that target. This way, the neural prosthesis continuously matched the master's planned target of movement with stimulation parameters/electrode locations that elicited movement in the avatar's limb to the same target. Importantly,

selected stimulation parameters and electrode contacts were set to produce limb movement that precisely reached and held the intended target in their two-dimensional space (Fig. 1).

As noted above, mean cross-validated performance during model training was $96 \pm 10\%$ when tested across training sessions with 854 training trials (Fig. 2b). We find that, when the masters performed the same task as before but target selection was controlled by joystick movements made by the avatar using the neural prosthetic, performance was slightly lower but still significantly higher than chance. Overall, the primates reached the displayed targets during these real-time recording-elicitation sessions in $84 \pm 14\%$ (mean \pm s.e.m.) of the 561 trials tested (binomial test, $P < 0.01$). Most incorrect trials (11%) occurred because of decoding error (i.e., selecting the wrong target). Only a few errors (5%) occurred because the avatar-controlled cursor failed to reach the spatial confines of the displayed target (i.e., to maintain the cursor location within the 0.75 radians or 8% screen-surface of the target for 100 ms).

No movements were made by the master during the decoding period, prior to the go-cue presentation (i.e., the trial would abort if any movement was made). To further confirm that no movements were made, we recorded electromyography (EMG) activity from the master as the task was being performed over one session (see *Methods*). We found no difference in activity during the decoding period, prior to the go-cue, between planned movements (t-test, $P = 0.53$; Fig. 6).

Motor Control Based on Adaptive Sensorimotor Responses

In many circumstances, such as in the setting of full motor paralysis, it may not be possible to train models based on the subject's natural movement. Also decoders trained on physical movement by the subjects may not accurately model the subjects' planned movement during direct neural prosthetic control^{32,33}, and consequently adaptive changes in neural activity may allow for improved performance over time. We tested this possibility by assigning individual neurons within the same pre-motor population (i.e. the same recording electrodes) to control the avatar's limb movement by volitionally modulating their activity. Similar to a sensorimotor conditioning approach described previously^{21,34,35}, we randomly selected individual neurons and assigned them to control the target of movement by naturally varying their firing activity from trial-to-trial as the monkeys performed the same real-time neural prosthetic task above. In particular, depending on whether the firing activity of the assigned individual neuron went above or below a fixed firing rate threshold, movement would be elicited to one of the two targets (see *Methods*). Importantly, the mapping between the neuron's firing activity and target location was chosen randomly, and no joystick was used by the master at any time (Fig. 7a).

Using this approach, we recorded from 40 population cells. During these recordings, the primates performed 580 trials over 5 sessions. Starting performance by the selected cells was $37 \pm 10\%$ (mean \pm s.e.m.) over the first 10 trials. Correct target selection, however, then rapidly improved, reaching an average performance of $77 \pm 12\%$ (two-tailed t-test, $n=5$; $P = 0.02$; Fig. 7b). Overall, it took the monkeys 28 ± 13 trials, or approximately 3 minutes, to reach statistical learning criterion (see *Methods*)^{36,37}. The highest noted asymptotic performance was 90%. The mean firing rate of selected cells remained the same over the

time course of these sessions when comparing the first and second half of the session (two-tailed t-test; $P = 0.88$) as did variance in their firing rates (two-tailed t-test; $P = 0.92$).

During these adaptive sessions, no joystick was given to the monkeys and no visible movement was noted during the task. To further confirm that no sub-threshold movements were being made, we recorded EMG activity from the master over one session. We found no change in EMG activity during selection of one target *versus* the other (area under the curve; two-tailed t-test, $p = 0.62$) and no difference in EMG activity before versus after target presentation (windows = 3000 ms; two-tailed t-test, $p = 0.33$; Fig. 8).

Response of Non-Selected Neurons During Adaptive Control

Since each selected neuron can only encode a binary response using this potential approach (i.e. high versus low threshold), we wanted to determine whether other neurons not involved in controlling movement respond similarly to the intended targets. This may, therefore, provide insight into the potential capacity of larger neural populations and distinct selected cells to adaptively direct movement to more than two targets at a time.

By simultaneously recording from multiple neurons during these sessions, we found that neighboring neurons in the pre-motor population displayed surprisingly little correspondence with the activities of the selected neurons. Thirty five pre-motor cells were recorded over the same 5 sessions in addition to the selected cells. However, none of the recorded cells demonstrated a significant correlation (either positive or negative) when comparing the time-varying firing rates of selected cells to the other non-selected cells (Pearson's correlation, $n=35$; $P > 0.05$). In other words, cells that were not selected to control movement did not consistently increase their firing activity when the activity of the selected cell increased during targeted movement or *vice versa* (note that these single cells were selected randomly from the population and the mapping between their firing rates and target selection was chosen arbitrarily). An example of two such cells is shown in Figure 7c (also, note that both cells still markedly fluctuated their activities from trial to trial). Similarly, there was little correlation in activity when considering variations in the firing activities across all pairings (mean correlation $r = -0.012 \pm 0.022$; mean \pm s.e.m.). These findings, therefore, suggested that cells in the population not directly assigned to controlling the movement do not necessarily co-vary their activities with the intended target during artificial motor control.

DISCUSSION

Achieving volitional control of one's own limb has been an important goal in the field of neural prosthetic development. Recent work has shown that the intended targets of movement or movement sequences can be inferred from primary motor and pre-motor neurons and that, even with a small number of recorded cells, it is possible to distinguish between multiple distinct planned targets in space^{8, 10, 28}. Based on this initial evidence, the basic question that we aimed to investigate was whether it is possible to couple, in real-time, the animal's intended target of movement with unconstrained (360 degree range of movement), stimulation-elicited limb movements to the same target confines in two-dimensional space and under full functional paralysis. While such a goal will require

continued technical innovation, as an initial proof of concept, we devised and tested a cortical-spinal neural prosthesis designed for controlling limb movements to two different small targets randomly positioned on a screen. We hypothesized that by focusing on the target of movement, rather than the ongoing planned trajectory, it may be possible to provide a simple solution for directing naturalistic limb movement to different targets in space.

Prior work has tackled the problem of controlling limb movement by inferring the ongoing planned trajectory of movement in real-time²⁰. While this approach demonstrated the remarkable ability to elicit movement over a given trajectory, it is presently limited to directing movement to a single, repeated target in space. Hence the applicability of such an approach to generating movement towards distinct targets is unclear. Here, using an alternate approach that allows the animal to control only the intended target locations of movement, we show that it possible to produce unconstrained limb movements to more than one precisely positioned target on a screen. While a range of angles and amplitudes of movements could be produced with only a few implanted spinal cord and muscle electrodes, it is likely that a larger number of electrodes and/or contact sites would be needed to allow for elicited movement to more than two targets. An obvious limitation, however, is that such an approach would not accurately mimic the precise intended trajectory of movement which may also be important under certain task settings^{7, 19}.

We also examined whether neurons, randomly selected from the population, could similarly control limb movement by volitionally modulating their activity, thus resulting in adaptive motor prosthetic control. In order to allow for comparison with the above decoding approach, we recorded from the same pre-motor microelectrodes and tested the same two target locations using the same task. We find that under this two-target setting, the animals learned to significantly improve the target acquisition accuracy over a fairly short time-period and were able to reach accuracies comparable to (albeit somewhat lower than) the decoding-based approach. Using this adaptive approach, we also examined how other non-selected neurons concomitantly changed their firing activities. Prior studies have demonstrated broad motor population responses to upcoming movements^{1-3, 38}, indicating that such neurons encode planned/intended movements as a concerted population-wide vector or function. A more recent important study has also shown that, when decoders were trained on the directional tuning of motor populations (i.e. using multiple neurons), neurons that were not directly involved in prosthetic control continued to modulate with the animal's movements but did so more weakly³⁹.

In agreement with these findings, we observe that individual neurons in the pre-motor cortex that are assigned to control the movement progressively modulated their activity with the intended targets. However, we also find that when motor control was assigned to individual neurons whose activity was mapped to movement arbitrarily, other surrounding cells did not consistently modulate their activity with the intended targets. While we used only a limited number of neurons recorded from small pre-motor populations, this finding suggests that it may be possible to orthogonally train more than one, and potentially multiple, single neurons to encode a different set of target locations. Therefore, either decoding- or adaptive-based approaches may be viable options for controlling such a target-based neural prosthetic

and may provide straight forward means for artificially generating goal-directed movements under direct cortical control.

Finally, to provide a model of paralysis in which to test present and future neural prosthetic approaches aimed at enabling limb movement in full paralysis, we introduced a novel two-primate setup for functionally paralyzing awake-behaving animals. This new technique was useful in that it provided a relatively simple way by which to dissociate all spinal cord pathways, and by which to test motor control without the influence of partially or completely preserved efferent/afferent circuitries⁴⁰. Recent studies, in particular, have demonstrated that providing proprioceptive and kinesthetic feedback to healthy subjects performing a BMI task can significantly improve the BMI accuracy. Such feedback, however, is lost in paralysis and cannot help BMI performance in paralyzed subjects^{26, 27}. This lack of proprioceptive feedback has been achieved in BMIs for control of external devices by partially restraining the animal's arm³³. However, in neural prosthetics aimed at controlling the limb, such an approach would not be possible and hence the two-primate setup can provide a useful model by which to test such neural prosthetics. An analogous approach for using the nervous system of one animal to control the nervous system of another has also recently been employed to relay motor commands and sensory-related information^{41, 42}. A limitation of the dual-monkey model is that the monkeys do not display all the same clinical features as truly chronically paralyzed animals such as muscle rigidity or autonomic dysreflexia⁴³. However, and perhaps as importantly, paralysis was reversible and was not associated with the extreme morbidity inherent to spinal cord paralysis.

METHODS

Dual-primate Spinal Cord Paralysis Model

Two adult male Rhesus macaques, ages 6–8 years old, were included in this study in accordance with IACUC guidelines and approved by the Massachusetts General Hospital institutional review board. Two monkeys were used to confirm reproducibility of results and neural-prosthesis performance. Each monkey, alternating in role for each session, acted either as the master or avatar. Here, the *master* was seated in a primate chair placed within a radiofrequency shielded recording enclosure (Crist Instrument Co Ltd, Damascus, MD). The masters' head was restrained using a head post, and a spout was placed in front of its mouth to deliver juice using an automated solenoid. A computer monitor which displayed the task was placed at eye level in front of the master.

The primate acting as the *avatar* was seated in a separate enclosure. Its upper limb was secured onto a 360 degree, free range-of-motion, spring-loaded, joystick that controlled a cursor displayed on the master's screen. A NI DAQ card (National Instruments, TX) was used for the I/O behavioral interface, and the behavioral program was run in Matlab (MathWorks, MA) using custom made software routines⁴⁴. On separate weeks, the two primates interchangeably acted as either the master or avatar. Therefore, if the primate was an avatar on a given week, we would use stimulation parameters and electrode locations specific to that monkey. Note that stimulation parameters that were previously demonstrated, during testing, to produce upward arm movement in avatar #1 may be different from parameters used in avatar #2.

Recording Multi-Electrode Implantation

Multiple recording silicone multi-electrode arrays (NeuroNexus Technologies Inc., MI) were chronically implanted in each monkey⁴⁵. A craniotomy was performed along the dorsal-lateral region of frontal lobe under standard stereotactic guidance (David Kopf Instruments, CA). After directly visualizing the cortical gyral pattern underlying the craniotomy, the arrays were implanted into the dorsal and medial aspects of the pre-motor cortex (Brodmann area 6). This area was implanted with 3–4 arrays in each monkey, with each array possessing 32 electrode contacts in a 4x8 configuration. Spacing between vertical contacts was 200 μm and horizontal contacts 400 μm .

Recordings began two weeks following surgical recovery. A Plexon multichannel acquisition processor was used to amplify and band-pass filter the neuronal signals (150 Hz – 8 kHz; 1 pole low-cut and 3 pole high-cut with 1000x gain; Plexon Inc., TX). Signals were digitized at 40 kHz and processed to extract action potentials in real-time by the Plexon workstation. Classification of the action potential waveforms was performed using template matching and principle component analysis based on waveform parameters. Only single-, well-isolated units with identifiable waveform shapes and adequate refractory periods were used for the on-line experiments and off-line analysis. No multiunit activity was used.

For electromyographic (EMG) recordings, we used tin surface electrodes from over the deltoid contralateral to neural recordings (this muscle displayed the most robust peri-movement activity during movement to both targets). Signals were digitized at 1 kHz and were recorded by the Plexon workstation.

Stimulating Electrode Implantation

Stimulating electrodes were chronically implanted in the cervical spinal cord of both monkeys. A dorsal skin incision was placed over the C5-6 lamina, and a laminectomy was performed to expose the dorsal spinal canal. In both avatars, two 16-contact iridium oxide stimulating electrode (100–500 k Ω) were inserted at the C5 and C6 levels (NeuroNexus Technologies Inc., MI). These were placed to a depth of 4 mm from the dorsal surface and 2 mm lateral from midline, corresponding to the approximate location of the ventral horn of the spinal cord. A fibrin sealant (Baxter, IL) was used to cover the dural opening, and the distal female connector was secured into place using a titanium mini-plate and acrylic cement along the lateral laminar edge. In addition to spinal cord electrode implantation, percutaneous electrodes (100–200 k Ω) were each placed, under sterile preparation, in the long and short head of the triceps muscle of avatar #1. The connecting wires were secured into place using an elastic cuff and attached to a female connector.

Behavioral Task

All trials during the task began with presentation of a circular green target that was randomly positioned in one of two locations on a screen (roughly, top versus bottom of the screen during avatar #1 sessions and top versus right of the screen during avatar #2 sessions). On decoding-based sessions, a go-cue would appear 1500 ms after target onset, following which time the master was allowed to move the joystick in order to guide a cursor from the center of the screen to the intended target. During real-time performance of the

recording-elicitation sessions, the exact same sequence of target presentations and go-cue timings would be given but, now, movement of the cursor would be based on joystick-attached limb movements made by the avatar. The master only received reward if the displayed target was reached and held for 100 ms.

Target Selection Based on Decoded Population Responses

We first inferred the planned target of movement in the master based on neural activities recorded in their pre-motor cortex. Using a population decoding approach, we determined the intended target of movement based on the firing activities of the neuronal population as masters performed the task. In order to estimate the masters' planned target of movement, we initially trained the models on the activity of neuronal populations in their pre-motor cortex as they performed the task using a joystick during the training sessions.

The spiking activity of each neuron was modeled as an inhomogeneous Poisson process whose likelihood function is given by;

$$p(N_{1:K}^c | S_i) = \prod_{k=1}^K (\lambda_c(k | S_i) \Delta)^{N_k^c} \exp(-\lambda_c(k | S_i) \Delta), \quad (1)$$

where Δ is the time increment taken to be small enough to contain at most one spike, N_k^c is the binary spike event of the c 'th neuron in the time interval $[(k-1)\Delta, k\Delta]$, $\lambda_c(k | S_i)$ is its instantaneous firing rate in that interval, S_i is the i 'th target of movement, and K is the total number of bins in a duration $K\Delta$. We take $\Delta = 5$ ms as the bin width of the spikes. For each target and neuron, we estimated the firing rate $\lambda_c(k | S_i)$ over the 1500 ms target presentation period (prior to the go cue) using a state-space expectation-maximization (EM) approach²⁸. After fitting the models, we validated them using the χ^2 goodness-of-fit test on the data and confirmed that they fitted the data well ($P > 0.7$ for all cells in all sessions). As noted in the main text, we had previously used such a decoding approach to infer the intended target of movement of primates across multiple targets and target sequences (i.e. up to 12). For the purpose of the present experiments, we decoded only two targets at a time.

During real-time recording-elicitation neural prosthetic experiments, the master's joystick was disconnected and the intended target of movement was inferred using a maximum-likelihood decoder based on neuronal activity recorded from the same premotor population. The maximum-likelihood decoder was used to determine the intended target based on the neuronal activity recorded over 1500 ms during the target presentation period and prior to the animals movement²⁸. Using the model above, the population likelihood under any target is given by;

$$p(N_{1:K}^{1:C} | S_i) = \prod_{c=1}^C \prod_{k=1}^K (\lambda_c(k | S_i) \Delta)^{N_k^c} \exp(-\lambda_c(k | S_i) \Delta) \quad (2)$$

where K is the total number of bins (300) during the target presentation period, C is the total number of neurons, and $\lambda_c(k | S_i)$ for $k = 1, \dots, K$ and $c = 1, \dots, C$ is the estimate of the firing rate. The decoded target was selected as the one that had the highest population likelihood. Finally, we evaluated the accuracy of the decoders obtained during the training session using

leave-one-out cross-validation. This allowed us to examine the accuracy of the trained models on a trial-by-trial basis.

Threshold and Target Determination on Adaptive Sessions

In a separate set of sessions, single neurons were individually selected from the same pre-motor population (i.e. recording electrode contacts) in the master and were randomly assigned to control limb movement produced by the avatar. These selected neurons were allowed to naturally vary their firing activity from trial-to-trial and, depending on whether their firing activity went above or below a fixed firing rate threshold, movement to one of the two possible target locations would be elicited. Importantly, the mapping between the neuron's firing activity, target location and elicited movement was chosen randomly. Moreover, unlike the decoding-based approach, no joystick was used by the master at any time⁴⁶.

With regards to determining the thresholds, prior to performing the recording-elicitation sessions, the natural firing rate distribution of the selected neuron was determined by recording its spiking activities while the master remained at rest for 5 minutes. Following this, the top 90th and bottom 10th percentiles of that distribution were determined. Each threshold was randomly assigned to correspond to selection of movement to one of the two displayed targets (e.g. reaching the low threshold could correspond to movement to the top target whereas reaching a high threshold could correspond to movement to the bottom target, or *vice versa*, on a given session). On each trial during the real-time recording-elicitation sessions, the firing rate of the same selected neuron would be calculated in 1000 ms windows advanced in 100 ms increments (i.e. total number of spikes counted over 1 second). If at any point after an initial 1500 ms delay the firing rate of the selected neuron reached either the top 90th or the bottom 10th percentile of their firing rate distribution, one of the two possible targeted movements would be elicited in the avatar. Reward would only be given to the master if the correct displayed target was reached and held for 100 ms (note that, since a target would be selected if either threshold was reached within a 1500 ms trial duration, there was only a 0.8¹⁵ chance that no movement would be elicited, meaning that movement was elicited in essentially all trials).

Statistical Testing

Correlated activity between selected and other non-selected neurons within the recorded pre-motor population was assessed based on their Pearson's product-moment coefficients ($P < 0.05$). Evaluating accuracy of behavioral performance above chance was assessed using a binomial test ($P < 0.05$), and change in performance across sessions was assessed by a two-tailed t-test ($P < 0.05$). All these values were given with their standard error of the mean (s.e.m). Behavioral performance was estimated from the animals' binary responses (correct versus incorrect target) using a Bernoulli state space approach described previously^{36,37}. Briefly, this was accomplished by fitting the curve to a standard logistic equation which provided a continuous estimate, ranging from 0 to 1, of the animals' learning performance. The 99% confidence bounds of the curve were used to determine when learning criterion was statistically achieved (i.e., when the confidence bounds first went above 50% chance). With regards to kinematics, the displacement and velocity of movements were calculated

from the trajectory tracings of each movement. The standard deviation of movement was determined by calculating the distance between each point along the trajectory of the cursor (i.e., as it curvilinearly moved from the center of the screen to the target) and that of the optimal trajectory (i.e. a straight line from the center of the screen to the center of the displayed target).

ACKNOWLEDGEMENTS

We thank E. Brown and E. Bizzi for their initial input into the project; K. Harous, M. Campos, J Pezaris and K. Spiliopoulos for their insightful discussion. We also greatly thank Marissa Powers who assisted with setting up the primate rig and with initial stimulation testing. R.C.U is funded by the NREF and Z.M.W is funded by NIH 5R01-HD059852, Presidential Early Career Award for Scientists and Engineers and the Whitehall Foundation.

REFERENCES

1. Alexander GE, Crutcher MD. Neural representations of the target (goal) of visually guided arm movements in three motor areas of the monkey. *J Neurophysiol.* 1990; 64:164–178. [PubMed: 2388063]
2. Georgopoulos AP, Kalaska JF, Caminiti R, Massey JT. On the relations between the direction of two-dimensional arm movements and cell discharge in primate motor cortex. *J Neurosci.* 1982; 2:1527–1537. [PubMed: 7143039]
3. Kakei S, Hoffman DS, Strick PL. Muscle and movement representations in the primary motor cortex. *Science.* 1999; 285:2136–2139. [PubMed: 10497133]
4. Paninski L, Shoham S, Fellows MR, Hatsopoulos NG, Donoghue JP. Superlinear population encoding of dynamic hand trajectory in primary motor cortex. *J Neurosci.* 2004; 24:8551–8561. [PubMed: 15456829]
5. Gardiner TW, Nelson RJ. Striatal neuronal activity during the initiation and execution of hand movements made in response to visual and vibratory cues. *Exp Brain Res.* 1992; 92:15–26. [PubMed: 1486949]
6. Wessberg J, et al. Real-time prediction of hand trajectory by ensembles of cortical neurons in primates. *Nature.* 2000; 408:361–365. [PubMed: 11099043]
7. Shanechi MM, et al. A real-time brain-machine interface combining motor target and trajectory intent using an optimal feedback control design. *PLoS One.* 2013; 8:e59049. [PubMed: 23593130]
8. Santhanam G, Ryu SI, Yu BM, Afshar A, Shenoy KV. A high-performance brain-computer interface. *Nature.* 2006; 442:195–198. [PubMed: 16838020]
9. Velliste M, Perel S, Spalding MC, Whitford AS, Schwartz AB. Cortical control of a prosthetic arm for self-feeding. *Nature.* 2008; 453:1098–1101. [PubMed: 18509337]
10. Musallam S, Corneil BD, Greger B, Scherberger H, Andersen RA. Cognitive control signals for neural prosthetics. *Science.* 2004; 305:258–262. [PubMed: 15247483]
11. Taylor DM, Tillery SI, Schwartz AB. Direct cortical control of 3D neuroprosthetic devices. *Science.* 2002; 296:1829–1832. [PubMed: 12052948]
12. Hochberg LR, et al. Neuronal ensemble control of prosthetic devices by a human with tetraplegia. *Nature.* 2006; 442:164–171. [PubMed: 16838014]
13. Prochazka A, Mushahwar VK, McCreery DB. Neural prostheses. *J Physiol.* 2001; 533:99–109. [PubMed: 11351018]
14. Tillery SI, Taylor DM. Signal acquisition and analysis for cortical control of neuroprosthetics. *Curr Opin Neurobiol.* 2004; 14:758–762. [PubMed: 15582380]
15. Jackson A, Moritz CT, Mavoori J, Lucas TH, Fetz EE. The Neurochip BCI: towards a neural prosthesis for upper limb function. *IEEE Trans Neural Syst Rehabil Eng.* 2006; 14:187–190. [PubMed: 16792290]
16. McKhann GM 2nd. Cortical control of a prosthetic arm for self-feeding. *Neurosurgery.* 2008; 63:N8–N9. [PubMed: 18797344]

17. Collinger JL, et al. High-performance neuroprosthetic control by an individual with tetraplegia. *Lancet*. 2013; 381:557–564. [PubMed: 23253623]
18. Carmena JM, et al. Learning to control a brain-machine interface for reaching and grasping by primates. *PLoS Biol*. 2003; 1:E42. [PubMed: 14624244]
19. Shanechi MM, Wornell GW, Williams ZM, Brown EN. Feedback-Controlled Parallel Point Process Filter for Estimation of Goal-Directed Movements from Neural Signals. *IEEE Trans Neural Syst Rehabil Eng*. 2012
20. Ethier C, Oby ER, Bauman MJ, Miller LE. Restoration of grasp following paralysis through brain-controlled stimulation of muscles. *Nature*. 2012; 485:368–371. [PubMed: 22522928]
21. Moritz CT, Perlmutter SI, Fetz EE. Direct control of paralysed muscles by cortical neurons. *Nature*. 2008; 456:639–642. [PubMed: 18923392]
22. Lemay MA, Galagan JE, Hogan N, Bizzi E. Modulation and vectorial summation of the spinalized frog's hindlimb end-point force produced by intraspinal electrical stimulation of the cord. *IEEE Trans Neural Syst Rehabil Eng*. 2001; 9:12–23. [PubMed: 11482358]
23. Giszter SF, Mussa-Ivaldi FA, Bizzi E. Convergent force fields organized in the frog's spinal cord. *J Neurosci*. 1993; 13:467–491. [PubMed: 8426224]
24. Mussa-Ivaldi FA, Giszter SF, Bizzi E. Linear combinations of primitives in vertebrate motor control. *Proc Natl Acad Sci U S A*. 1994; 91:7534–7538. [PubMed: 8052615]
25. Bizzi E, Mussa-Ivaldi FA, Giszter S. Computations underlying the execution of movement: a biological perspective. *Science*. 1991; 253:287–291. [PubMed: 1857964]
26. Suminski AJ, Tkach DC, Fagg AH, Hatsopoulos NG. Incorporating feedback from multiple sensory modalities enhances brain-machine interface control. *J Neurosci*. 2010; 30:16777–16787. [PubMed: 21159949]
27. Hatsopoulos NG, Suminski AJ. Sensing with the motor cortex. *Neuron*. 2011; 72:477–487. [PubMed: 22078507]
28. Shanechi MM, et al. Neural population partitioning and a concurrent brain-machine interface for sequential motor function. *Nat Neurosci*. 2012; 15:1715–1722. [PubMed: 23143511]
29. Mushahwar VK, Gillard DM, Gauthier MJ, Prochazka A. Intraspinal micro stimulation generates locomotor-like and feedback-controlled movements. *IEEE Trans Neural Syst Rehabil Eng*. 2002; 10:68–81. [PubMed: 12173741]
30. Moritz CT, Lucas TH, Perlmutter SI, Fetz EE. Forelimb movements and muscle responses evoked by microstimulation of cervical spinal cord in sedated monkeys. *J Neurophysiol*. 2007; 97:110–120. [PubMed: 16971685]
31. Zimmermann JB, Seki K, Jackson A. Reanimating the arm and hand with intraspinal microstimulation. *J Neural Eng*. 2011; 8:054001. [PubMed: 21828907]
32. Ganguly K, Carmena JM. Emergence of a stable cortical map for neuroprosthetic control. *PLoS Biol*. 2009; 7:e1000153. [PubMed: 19621062]
33. Carmena JM. Advances in neuroprosthetic learning and control. *PLoS Biol*. 2013; 11:e1001561. [PubMed: 23700383]
34. Moritz CT, Fetz EE. Volitional control of single cortical neurons in a brain-machine interface. *J Neural Eng*. 2011; 8:025017. [PubMed: 21436531]
35. Fetz EE. Operant conditioning of cortical unit activity. *Science*. 1969; 163:955–958. [PubMed: 4974291]
36. Williams ZM, Eskandar EN. Selective enhancement of associative learning by microstimulation of the anterior caudate. *Nat Neurosci*. 2006; 9:562–568. [PubMed: 16501567]
37. Wirth S, et al. Single neurons in the monkey hippocampus and learning of new associations. *Science*. 2003; 300:1578–1581. [PubMed: 12791995]
38. Georgopoulos AP, Schwartz AB, Kettner RE. Neuronal population coding of movement direction. *Science*. 1986; 233:1416–1419. [PubMed: 3749885]
39. Ganguly K, Dimitrov DF, Wallis JD, Carmena JM. Reversible large-scale modification of cortical networks during neuroprosthetic control. *Nat Neurosci*. 2011; 14:662–667. [PubMed: 21499255]
40. Luce JM. Medical management of spinal cord injury. *Crit Care Med*. 1985; 13:126–131. [PubMed: 3881221]

41. Yoo SS, Kim H, Filandrianos E, Taghados SJ, Park S. Non-invasive brain-to-brain interface (BBI): establishing functional links between two brains. *PLoS One*. 2013; 8:e60410. [PubMed: 23573251]
42. Pais-Vieira M, Lebedev M, Kunicki C, Wang J, Nicolelis MA. A brain-to-brain interface for real-time sharing of sensorimotor information. *Sci Rep*. 2013; 3:1319. [PubMed: 23448946]
43. Karlsson AK. Autonomic dysreflexia. *Spinal Cord*. 1999; 37:383–391. [PubMed: 10432257]
44. Asaad WF, Eskandar EN. Achieving behavioral control with millisecond resolution in a high-level programming environment. *J Neurosci Methods*. 2008; 173:235–240. [PubMed: 18606188]
45. Nicolelis, MAL. *Methods for neural ensemble recordings*. Edn. 2. Boca Raton, FL: Frontiers in Neuroscience; 2008.
46. Koralek AC, Jin X, Long JD 2nd, Costa RM, Carmena JM. Corticostriatal plasticity is necessary for learning intentional neuroprosthetic skills. *Nature*. 2012; 483:331–335. [PubMed: 22388818]

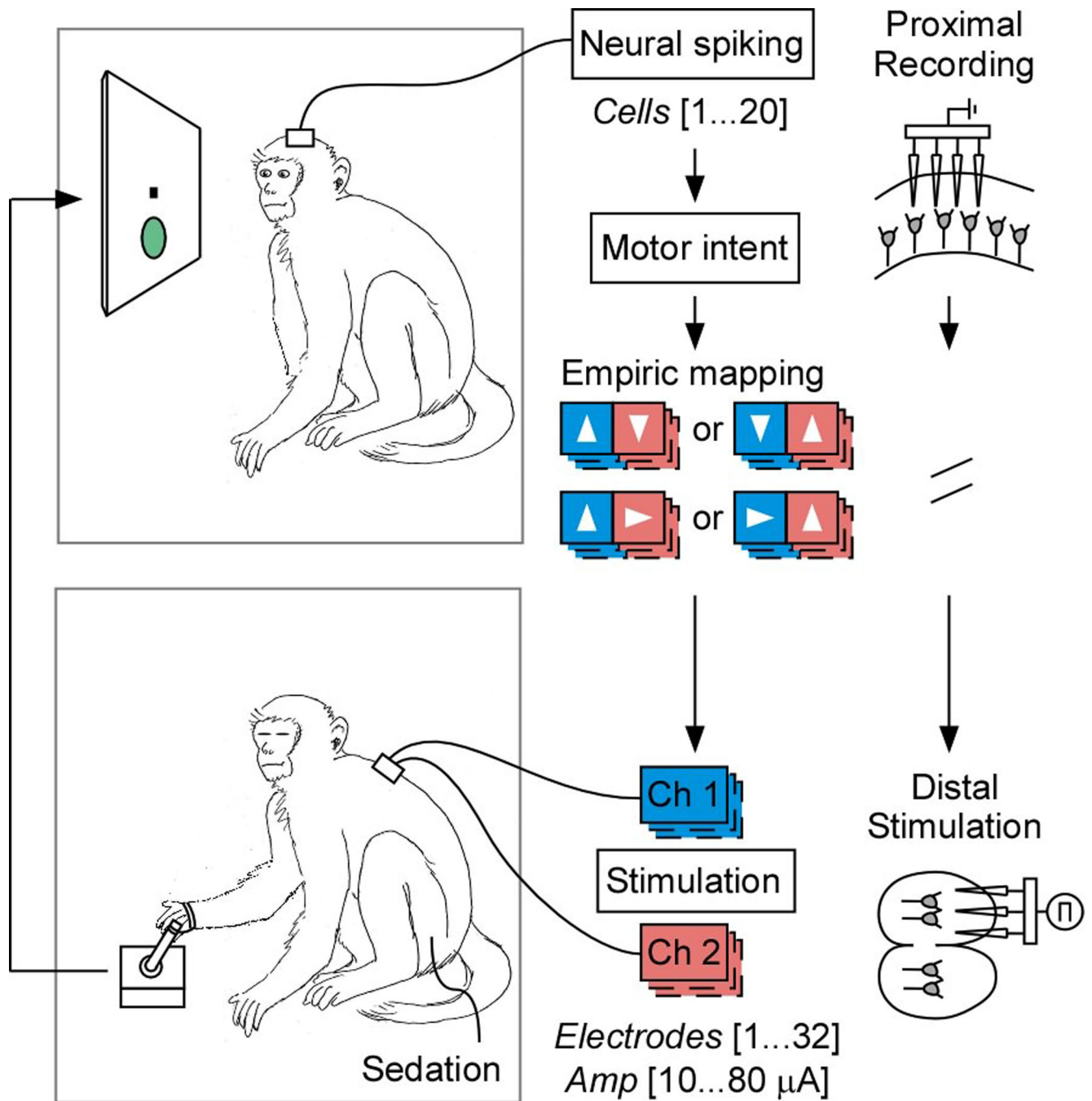


Figure 1. Schematic illustration of the dual-primate set up. The master is displayed on *top* and the avatar is displayed on the *bottom*. Note that on decoding-based sessions, the master had a joystick during training that was then disconnected during the real-time neural prosthetic trials. On adaptive-based sessions, no joystick was used at any time. Under “empiric mapping”, the arrows indicate the estimated intended target of movement based on neural activity and the color codes illustrate the corresponding stimulator channel used to elicit

limb movement in the animal. The left vs. right pairings indicate the two possible mappings to movement to each of the targets for the first and second avatars, respectively.

Author Manuscript

Author Manuscript

Author Manuscript

Author Manuscript

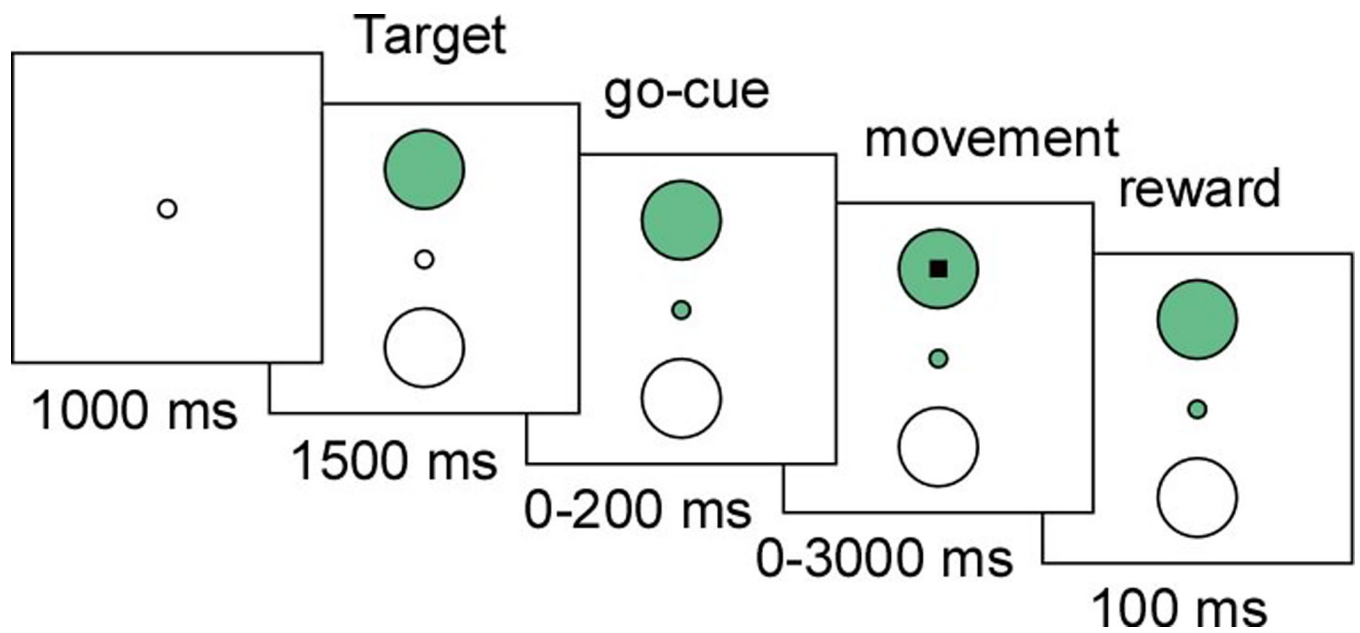


Figure 2. Behavioral task. Schematic illustration of the trial presentation and timeline proceeding from left to right. On decoding based sessions, a central green circle was used as a go-cue. On adaptive, single-neuron based sessions, no go-cue was given. Only the displayed target is shown on this particular trial (i.e. the other possible target/movement locations are not shown). During model training and adaptive sessions, the monkeys had up to 3000 ms to make a movement.

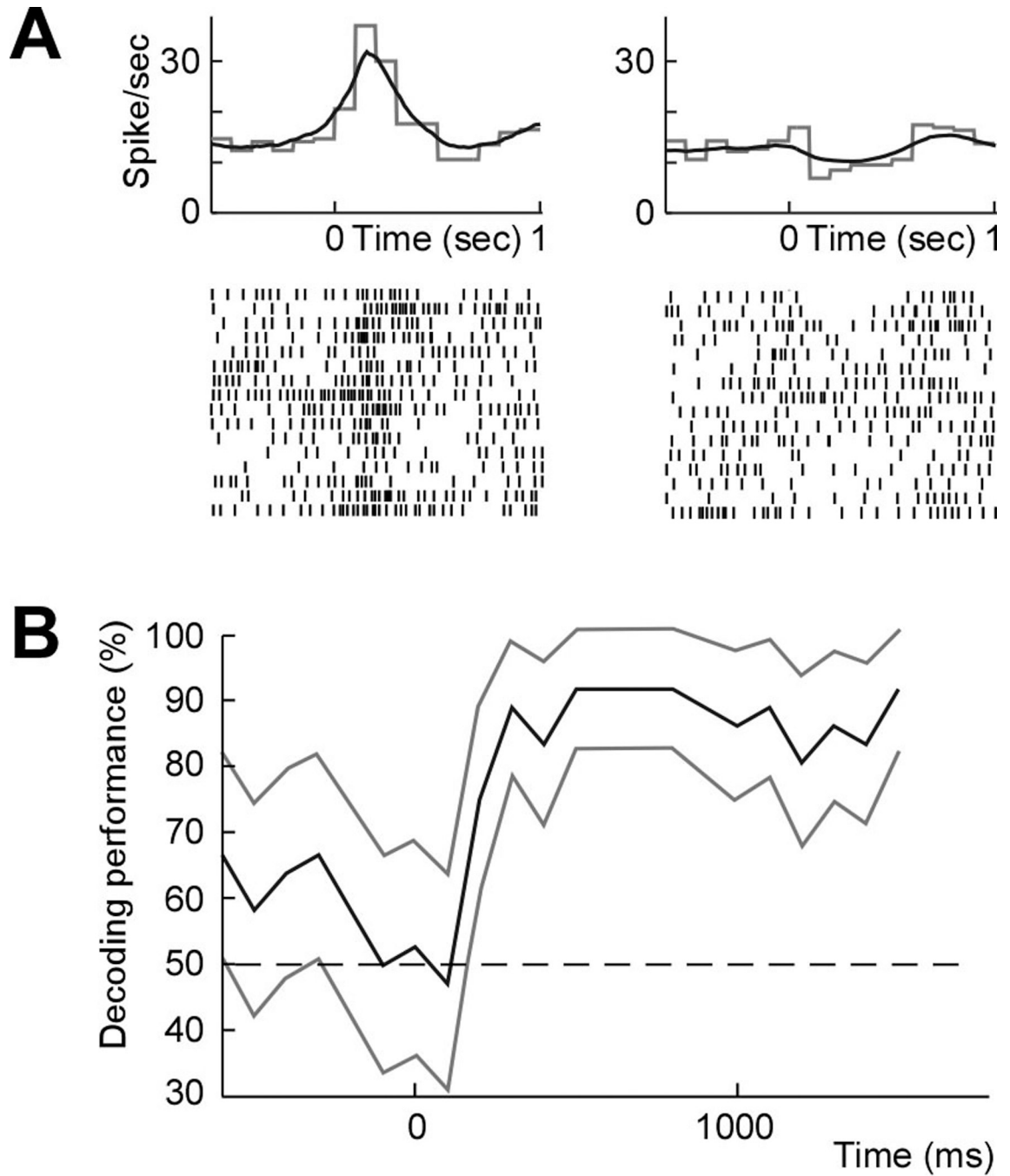


Figure 3. Neural population decoding. **(a)** Averaged (gray) and model estimated (black) peristimulus histogram (*top*) and raster (*bottom*) of a pre-motor neuron during movement planning and aligned to presentation of two different targets (*left* and *right*, respectively). **(b)** Mean population decoding performance across all trials and 95% confidence bounds aligned to target presentation (and up to the go-cue) during a sample session.

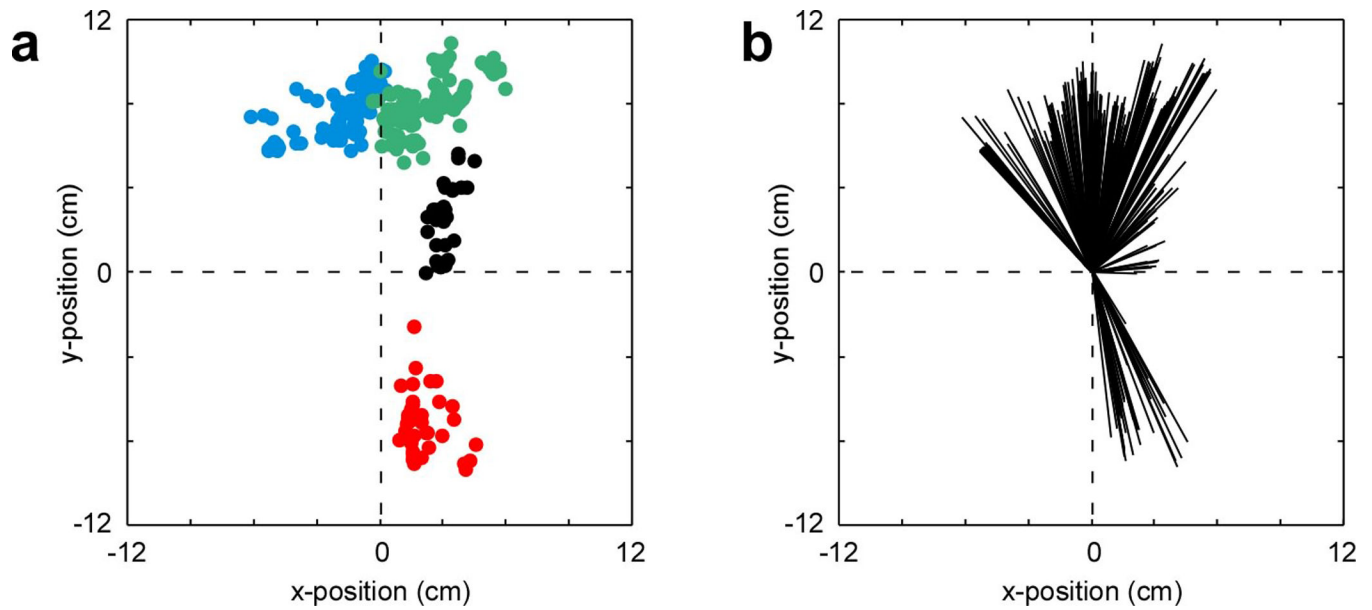


Figure 4.

Microstimulation-induced limb movement during testing. (a) Scatter plot indicating the mean cursor position during the last 100 ms of stimulation (during which the target was held) for all tested electrode sites. These together define the possible range of movements elicited in the two avatars during testing. For avatar #1, blue dots indicate the end-targets of movement produced by C5 electrode stimulation and red dots indicate the end-targets of movement produced by triceps stimulation. For avatar #2, green dots indicate the end-targets of movement produced by C5 electrode stimulation and black dots indicate the end-targets of movement produced by C6 stimulation. (b) Distribution of elicited movement directions in relation to center.

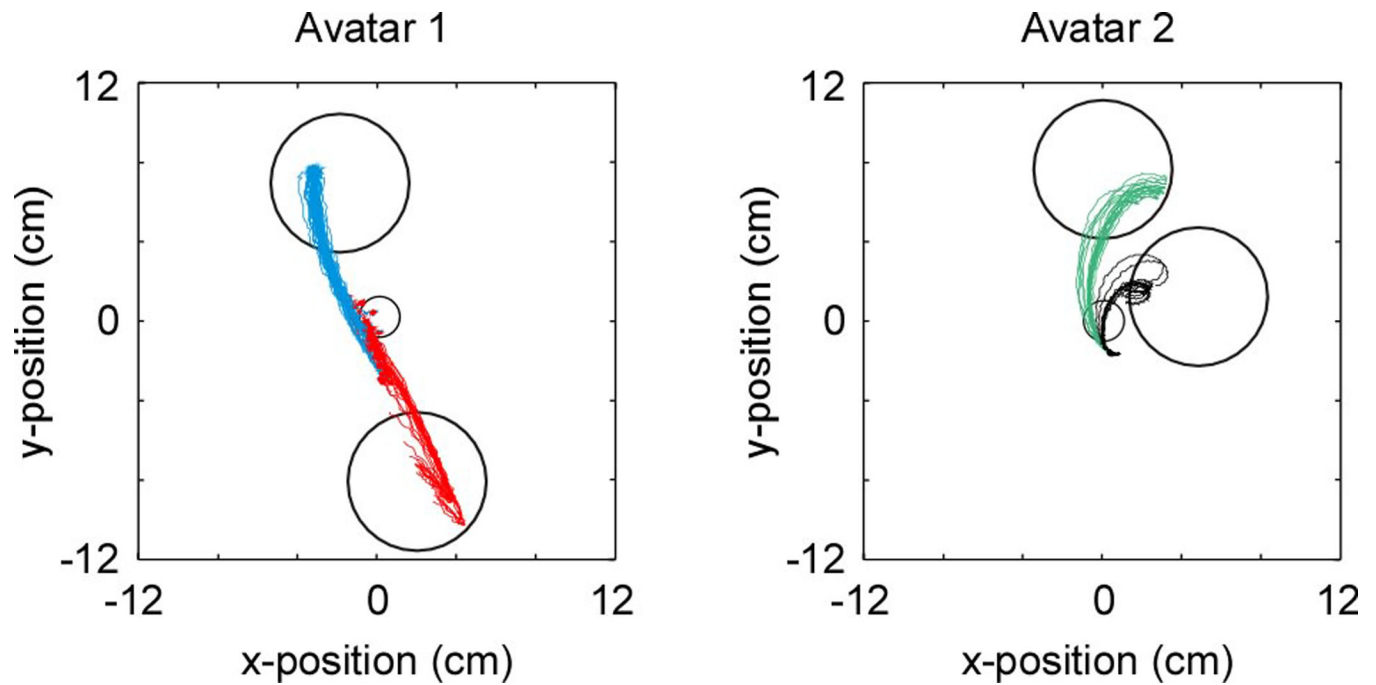


Figure 5. Selected targets and elicited limb movement trajectories used for the real-time sessions. Target locations and the stimulation-induced limb movement trajectories are shown for avatar #1 (*left*) and avatar #2 (*right*). For avatar #1, upwards movements (blue) were produced by C5 electrode stimulation and downward movements (red) by triceps stimulation. For avatar #2, upwards movements (green) were produced by C5 electrode stimulation and righthward movements (black) by C6 stimulation.

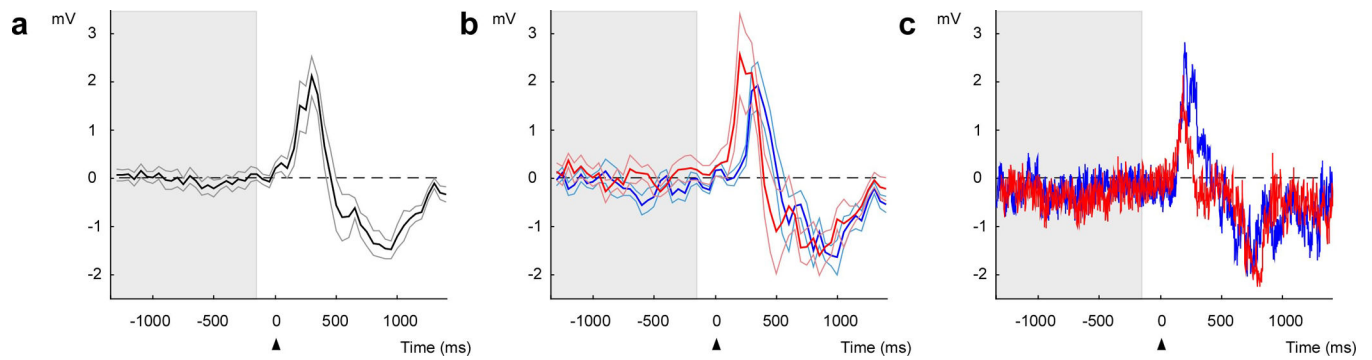


Figure 6.

EMG tracings display robust peri-movement activity during movement to both targets. **(a)** Averaged EMG tracings in millivolts over the course of a real-time recording-elicitation session. The gray area indicates the time during which neural decoding was performed and the arrow (time zero) indicates the time of the go-cue. The thick line indicates the average activity and the thin lines the s.e.m. **(b)** EMG tracings are broken down into target of movement (red for *up* and blue for *right*). **(c)** Raw EMG tracings over two individual trials with the same color convention as in **b**.

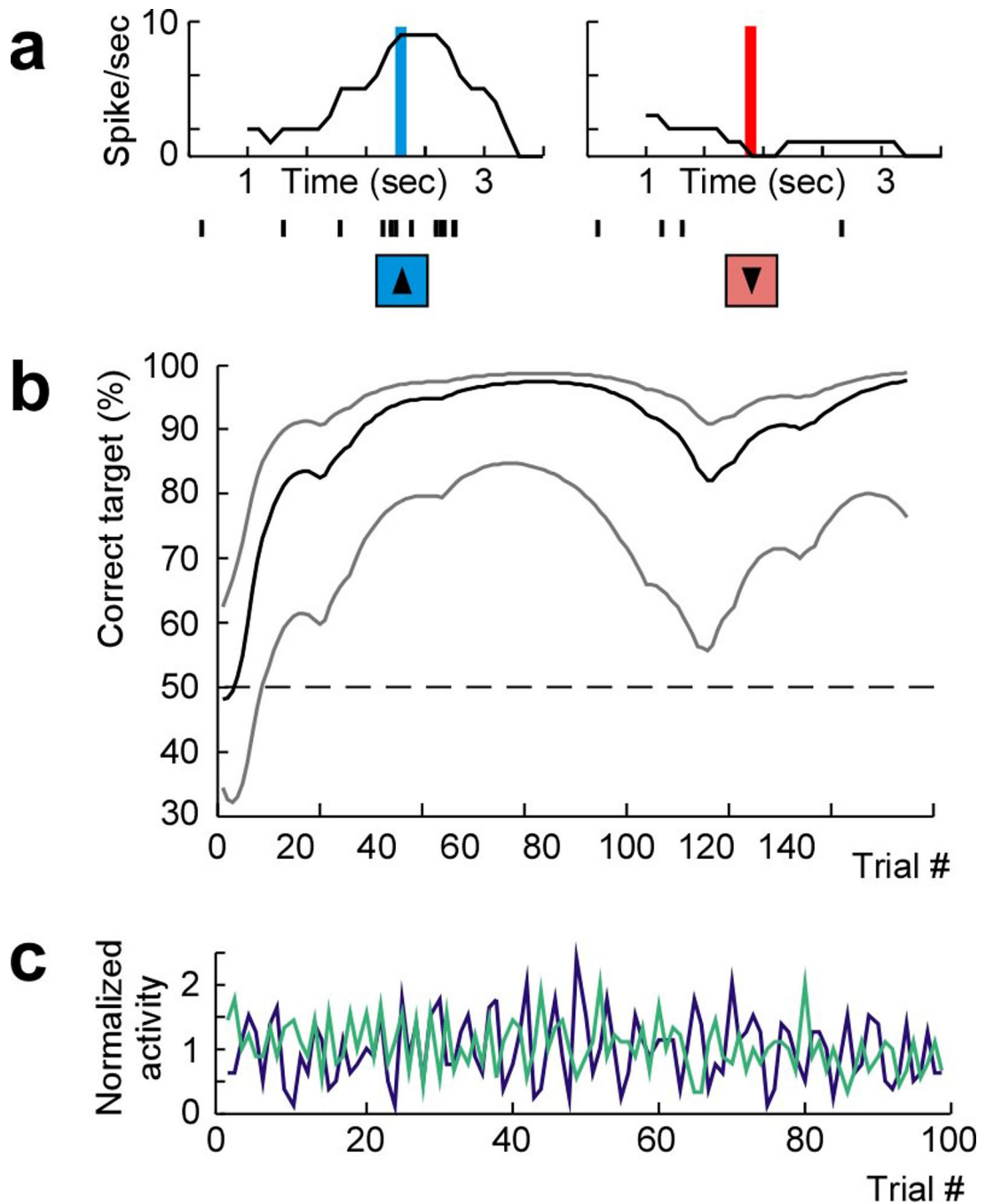


Figure 7.

Adaptive activity based approach for controlling movement. **(a)** The firing rate and corresponding spike time indicators (immediately below the x-axis) of a single selected premotor neuron recorded over two individual trials aligned to target presentation for two different targets. The vertical bars indicate the time during which the firing rate of the neuron reached the top threshold (*left*, blue) and bottom threshold (*right*, red; see Methods for further detail on threshold definition). The arrows indicate the time of stimulation and mapped elicited limb movement for each trial. **(b)** Behavioral performance and 99%

confidence bounds over successive trials within a session (100% performance indicates that the primates correctly selected and spatially reached the displayed target on all trials). (c) Example of the normalized firing activities (averaged firing rate within successive 1000 ms windows divided by the mean firing rate across the entire session) of a selected (green) and a non-selected (purple) pre-motor neuron recorded over a single representative session.

Author Manuscript

Author Manuscript

Author Manuscript

Author Manuscript

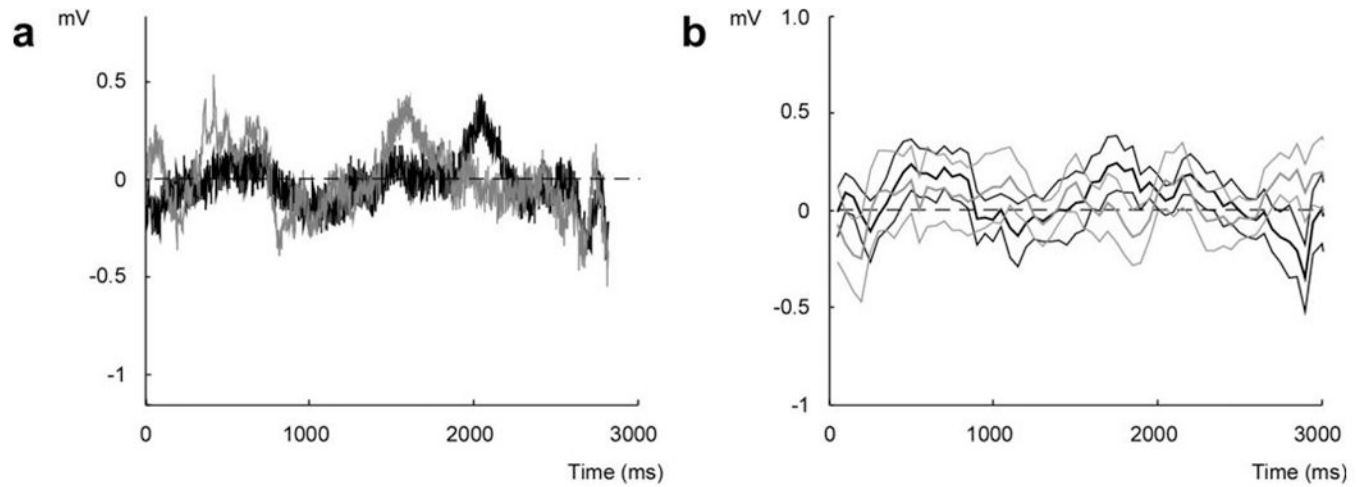


Figure 8.

EMG tracings in the master during the real-time adaptive recording-elicitation sessions. (a) An example of raw EMG tracings recorded in the master over individual trials during selection of the *top* (black) vs. *bottom* (gray) target. In both trials, the window over which neuronal threshold was reached lied between 1500-2500 ms. (b) Average EMG activity for all top vs. bottom movements over the course of the session, with the same color convention as in a. The thick lines indicate the mean EMG activity in millivolts and the thin lines indicate their s.e.m.